ELSEVIER

Polymer 41 (2000) 5109–5124

polymer

Endgroup substituent effects on the rate/extent of network formation and adhesion for phenylethynyl-terminated poly(arylene ether sulfone) oligomers

A. Ayambem, S.J. Mecham, Y. Sun, T.E. Glass, J.E. McGrath*

Chemistry Department and NSF Science and Technology Center for High Performance Polymeric Adhesives and Composites, Virginia Polytechnic Institute and State University, 2108 Hahn Hall, Blacksburg, VA 24061-0344, USA

Received 25 January 1999; received in revised form 8 July 1999; accepted 30 July 1999

Abstract

A series of poly(arylene ether sulfone) thermosets were synthesized from oligomers (M_n = 4–8000 g/mol) endcapped with various phenylethynyl moieties which differ in their electron-withdrawing abilities of their attached substituent. ^{13}C NMR showed that the nature of the substituent (e.g. ether, ketone, sulfone, imide) influences the electron density around the ethynyl bond, as well as the terminal phenyl-ring carbon atoms. Kinetic studies on the rate of cure at 320 and 350°C were conducted using FTIR, and in both cases the rate laws approximated second-order reactions at low to moderate conversions of the ethynyl bond. The rate of the curing reaction was observed to increase with the electron-withdrawing ability of the substituent on the phenylethynyl endcapper Glass transition temperatures (T_g) and the elastic modulus above the T_g of the networks increased with increasing electron-withdrawing ability of the substituent. Cured materials were solvent resistant and all formed tough creasable films, even when the oligomer M_n was as low as 4000 g/mol. The adhesive strengths of the cured materials were studied by Ti–Ti lap shear tests, and excellent values comparable to those of control polyimides, 5329 psi (37 MPa), were recorded. Interestingly, under constant curing conditions, the values obtained increased with the electron-withdrawing ability of the reactive endgroup.

Keywords: Arylene ether sulfone; Phenylethynyl; Thermoset

1. Introduction

Poly(arylene ether sulfones) and related materials are normally linear high performance engineering polymers which display a variety of desirable properties including thermal and dimensional stability, toughness, retention of modulus at high temperatures and, radiation resistance [1–23]. In spite of these desirable properties, they have been limited in their applicability in certain areas, because of their relatively poor solvent resistance. For instance, the fact that they undergo crazing and cracking in the presence of such organic liquids as jet fuel, hydraulic fluids (tricresyl phosphate), and de-icing fluids (ethylene glycol) has limited their use as structural adhesives and composite matrices in the aerospace industry. Reactive poly(arylene ether sulfone) oligomers such as (**I**) have been synthesized with terminal or pendant phenylethynyl endgroups which are sites for network formation to circumvent this drawback [9–11].

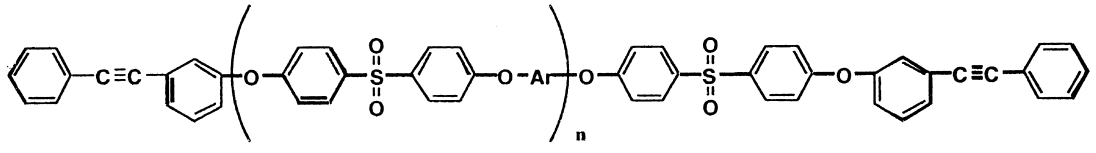

(I)

* Corresponding author. Tel.: +1-540-231-4457; fax: +1-540-231-8517.
E-mail address: jmcgrath@vt.edu (J.E. McGrath).

0032-3861/00/$ - see front matter
PII: S0032-3861(99)00573-X

The resulting thermosets exhibited high solvent resistance while maintaining many of the desirable properties of the corresponding high-molecular-weight thermoplastic material. The choice of the phenylethynyl moiety as endcapper was partially defined by its ability to react without the evolution of volatiles, which reduce adhesive and other mechanical properties. In addition, the phenylethynyl group only reacts rapidly at very high temperatures (above 350°C) [8–12] which are well above the glass transition temperatures of the oligomers. This allows a desirably large processing window for these materials, which is critical for the wetting and flow to develop properties necessary in the manufacture of structural adhesives and polymer matrix composites.

Previous studies of cured phenylethynyl-terminated poly (arylene ether sulfone) oligomers afforded network glass transition temperatures which were only about 0–5°C above those of the high-molecular-weight thermoplastics [8–23]. This relatively small increase was in contrast to analogous phenylethynyl-terminated polyimides which displayed glass transition temperatures that were nearly 50°C above the values of control high-molecular-weight thermoplastics [15]. These differences could be a function of crosslink density that might depend on the electronic environment around the phenylethynyl group. Although the exact mechanism is still not known, model studies of the curing reaction [16,17] have nonetheless generally suggested that the reaction proceeds by oligomeric chain extension and branching prior to crosslinking. Therefore, different electronic environments around the reactive phenylethynyl endgroup (e.g. electron donating or withdrawing) may influence the cure reaction in a particular direction by facilitating one process over another. This could affect the molecular weight between crosslinks (M_c) of the resulting thermoset, the glass transition temperature and perhaps other mechanical properties. Previous studies examining the effect of the nature of the substituent on the curing characteristics of the phenylethynyl group [18] revealed that electron-withdrawing substituents not only reduced the cure temperatures, but also accelerated the curing process. The importance of the glass transition temperature for high-performance applications, e.g. as aerospace structural adhesives, is well known, as the material might have to be durable at the standard operating temperatures, which for supersonic aircraft can be between 177–204°C for 60,000 h [19]. It has been proposed that for a material to withstand these conditions, it would have to have a minimum T_g of about 250°C. The literature T_g values for linear high molecular weight bisphenol-A based polysulfone thermoplastic is 190°C, whereas those for the biphenol-based system is 230°C [20,21], which suggests that a moderate crosslink density in the latter system might achieve the desired value of 250°C.

This article describes the synthesis and characterization studies which have further investigated the role of the electronic environment of the phenylethynyl endgroup of poly (arylene ether sulfone) oligomers on the cure kinetics, the thermal transitions and adhesion properties of the resulting cured material to titanium adherends.

2. Experimental section

2.1. Materials

Bisphenol-A of monomer grade purity (Dow Chemical) was dried at 80°C overnight under vacuum before use. The highly purified activated halide, 4,4′-dichlorodiphenylsulfone (DCDPS), (Amoco Chemical) and 4,4′-biphenol, (Aldrich Chemicals) were dried at 80°C under vacuum overnight before use. An endcapper, 3-aminophenol (Aldrich Chemicals) was recrystallized twice from toluene and then dried under vacuum at 60°C for 12 h before use. Potassium carbonate (Fisher Scientific) was dried at 130°C under vacuum. The phenylethynyl phthalic anhydride was synthesized by the reaction of 4-bromophthalic anhydride with phenylacetylene [9–11,16] *N*-Methyl-pyrollidone (NMP) and *o*-dichlorobenzene (*o*-DCB) (Fisher Scientific) were dried over calcium hydride and distilled under vacuum before use. Toluene (Fisher Scientific) was used as received.

The endcapper 4-fluoro-4′-phenylethynyl-4-benzophenone (FPEB) was kindly provided by Dr John W. Connell (NASA Langley) and was used after drying under vacuum at 80°C overnight, m.p. = 151°C.

2.2. Endcapper synthesis

2.2.1. Synthesis of 3-phenylethynylphenol

2.2.1.1. Protection of 3-bromophenol To a 500 ml three-neck round bottom flask with a condenser, magnetic stir bar and nitrogen flow was added 70.5 g 3-bromophenol (0.407 mol) and 115 ml acetic anhydride (1.22 mol). The reaction mixture was stirred, placed in an oil bath and allowed to reflux at 145°C for 2 h, after which it was removed from the bath and cooled. The light yellow solution was transferred to a 1 l Erlenmeyer flask and 2 × 250 ml portions of distilled water were added slowly with stirring. After cooling to ambient temperature, the solution was extracted with 4 × 400 ml of diethyl ether. The combined ether layers were washed with 4 × 500 ml and 3 × 1 l of distilled water to remove any remaining acetic acid or acetic anhydride. The ether was then removed by rotary evaporation to provide pure 3-bromophenylacetate.

2.2.1.2. Oxidative addition of phenylacetylene and 3-bromophenylacetate A 1 l three-neck round bottom flask was fitted with a condenser, overhead stirrer and nitrogen inlet and flamed dried under a nitrogen atmosphere. Next, 84 93 g of 3-bromophenylacetate (0 395 mol), 51 99 g of phenylacetylene (0.509 mol) and 0 963 g of triphenylphosphine (0.0037 mol) were added into the reaction vessel with 530 ml of triethylamine. Stirring was

started, and the remainder of the reaction steps were conducted in the dark. 0.471 g of bis(triphenylphosphine)palladium (II) chloride (0.0007 mol) and 0.190 g of copper(I) iodide (0.001 mol) were then added into the reaction vessel along with 30 ml of triethylamine. The reaction was heated to 120°C and stirred for about 12 h after which the resulting white precipitate was filtered and washed with triethylamine. The yellow filtrate was placed in a rotary evaporator and reduced to a brown oil which slowly crystallized, affording the crude 3-phenylethynylphenylacetate.

2.2.1.3. Deprotection of crude 3-phenylethynylphenylacetate Into a 1 l round bottom flask equipped with an overhead stirrer, condenser and nitrogen inlet was added 120 g of 3-phenylethynylphenylacetate (0 5 mol), 120 g of potassium carbonate (0 87 mol) and 600 ml of methanol. The reaction was allowed to reflux in a 90°C oil bath for 4 h and was subsequently cooled and isolated by addition of water. The resulting mixture was then concentrated by rotary evaporation, affording a biphasic oil/water solution, into which aqueous hydrochloric acid (0.2%) was slowly added until the pH was reduced to about 9. The oil solidified facilitating filtration from the water. Extraction of the water layer with ether and subsequent rotary evaporation of the ether afforded a dark oil which slowly crystallized. Both crude forms of the 3-phenylethynylphenol (3-PEP) product were purified by recrystallization with large amounts of hexanes to afford white crystals of pure 3-PEP (m.p. = 85–86°C).

Elemental analysis, calcd.: C, 86.57; H, 5.1; O, 8.24. Found: C, 86.50; H, 5.22; O, 7.80.

2.2.2. Synthesis of 4-fluoro-4′-phenylethynyldiphenylsulfone

2.2.2.1. Synthesis of 4-bromo-4′-fluorodiphenylsulfone To a 100 ml three-neck round bottom flask equipped with a overhead stirrer, nitrogen inlet and a water condenser with needle sized nitrogen outlet was added 15.3711 g of solid 4-fluorobenzenesulfonylchloride (0.07893 mol) and 30 ml of bromobenzene (0.28487 mol) as solvent. Next, 10.7344 g of aluminum chloride (0.08050 mol, 2 mol% excess) was added slowly, with no visible exotherm. The reaction flask was purged with nitrogen and placed in an oil bath at 140°C for 48 h. The reaction was cooled and added to 300 ml of hydrochloric acid/ice water and stirred. Solvent extraction was then effected using chloroform. The chloroform portion was rotovapped to give an orange liquid which slowly crystallized to a solid. The orange solid was recrystallized in hexanes containing charcoal to provide 10.6167 g (0.03369 mol) of 4-bromo-4′-diphenylsulfone. The dried white crystals were obtained in a yield of 66%.

2.2.2.2. Oxidative addition of 4-bromo-4′-fluorodiphenylsulfone and phenylacetylene To a flamed and purged 250 ml three-necked round bottom flask equipped with an overhead stirrer, condenser with nitrogen inlet and outlet was added 11.8594 g of 4-bromo-4′-fluorodiphenylsulfone (0.03763 mol), 0.0918 g of triphenylphosphine (0.0003499 mol) and 30 ml of triethylamine. Next, 5.37 ml of phenylacetylene (0.04890 mol) was added into the reaction vessel along with 15 ml of dry NMP. This was followed by the addition of 0.0449 g of bis(triphenylphosphine)palladium (II) chloride (0.00006 mol) and 0.0179 g of copper(I) iodide (0.00009 mol), in the dark, with 20 ml of triethylamine. The reaction was stirred, purged, and heated at 60°C for 12 h (in the dark), then cooled and filtered. The solid was washed with diethyl ether into the filtrate and placed in a rotary evaporator to remove the bulk of the solvent. The semi-solid material remaining was dried at 80°C in a vacuum oven affording crude 4-fluoro-4′-phenylethynyldiphenylsulfone powder. This powder was dissolved in 100 ml chloroform and washed with 4 × 100 ml of distilled water in a separatory funnel to remove the salt. Dropwise addition of hexanes to the chloroform solution promoted crystallization. The pure white crystals obtained were filtered and dried at 80°C in the vacuum oven (m.p. = 189°C).

Elemental analysis, calcd.: C, 71.41; H, 3.90; O, 9.51; S, 9.53; F, 5.65. Found: C, 71.61; H, 3.91; O, 9.20; S, 10.39; F, 5.31.

2.2.3. Synthesis of 4-phenylethynylphthalimidophenol

To a 100 ml three-neck round bottom flask equipped with a overhead stirrer, nitrogen inlet and a toluene filled dean stark trap with a condenser was added 10.1008 g of 3-phenylethynylphthalic anhydride (0.040284 mol) and 4.8895 g of 4-aminophenol (0.0443124 mol) with 30 ml of DMAc and 25 ml of toluene. The reaction vessel was kept under a nitrogen purge, stirred and placed in an oil bath at 170°C. Toluene (15 ml) was removed to increase the refluxing temperature to 145°C. After 6 h, the reaction was cooled, filtered, and washed with 1 l of diethyl ether to provide a light yellow solid which was dried in the vacuum oven at 120°C overnight. The crude PEPIP was dissolved in a 95/5 (v/v) mixture of chloroform and trifluoroacetic acid (TFA). This solution was immersed in an ice water bath and cyclohexane was added dropwise to induce crystallization of the pure product (m.p. = 283°C).

Elemental analysis, calcd.: C, 77.87; H, 3.86; N, 4.13; O, 14.14. Found: C, 77.14; H, 3.84; N, 4.10; O, 13.65.

2.3. Characterization

The oligomers were characterized by ^{1}H and ^{13}C NMR, thermal gravimetric analysis (TGA), differential scanning calorimetry (DSC), gel permeation chromatography (GPC or SEC), infrared spectrometry, and lap shear tests to measure adhesive properties of the thermosets. The number average molecular weights, M_n, were also obtained by

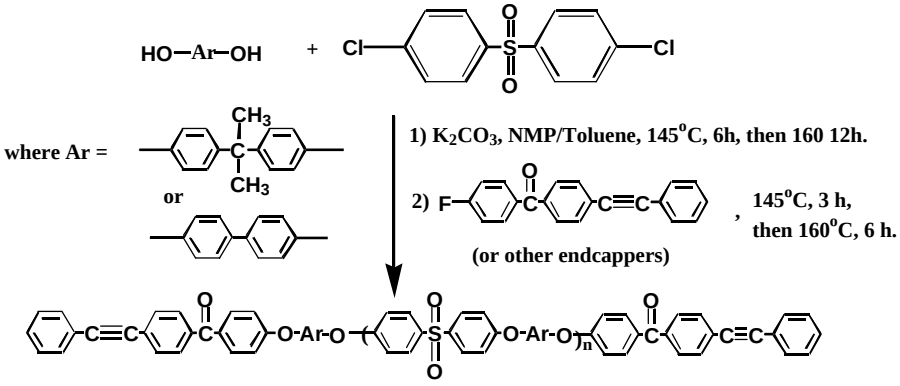

Scheme 1.

endgroup analysis through quantitative ^{1}H and ^{13}C-NMR . Quantitative ^{13}C-NMR spectra were run for 120 min with a spectral width of 25,000 Hz and a relaxation delay of 18.8 s, measured on a Varian Unity 400 NMR spectrometer. Elemental analyses were determined by Galbraith Laboratories, Inc. A Perkin–Elmer TGA-7 was employed to determine weight loss behavior in air. A Perkin–Elmer DSC-7 was used to identify the thermal transitions of the oligomers and cured network materials. DMA analysis were carried out by three point bending on a Perkin–Elmer DMA 7e instrument at a frequency of 1 Hz and a scanning rate of 3°C/min from −150 to 0°C, and at 5°C/min from 0 to 350°C. Absolute molecular weight measurement of polymers was conducted with a Waters 2690 separations module equipped with a differential refractometer detector and an on-line differential viscometric detector (Viscotek T60A) coupled in parallel. Waters microsyragel HR05 + HR2 + HR3 + HR4 column band were used. The mobile phase was NMP, containing 0.02 M P_2O_5. The flow rate was 1.0 μl/min, the injection volume was 100 ml, the column temperature was 60°C, and the polymer concentration was approximately 3 mg/ml. TriSec GPC Software V3.0 (Viscotek) was used to acquire and analyze the data. A series of narrow molecular weight distribution polystyrene standards (Polymer Laboratory) was employed to generate the universal calibration curve. Gel fractions were obtained from soxhlet extraction of the cured sample for 96 h with chloroform. The extracted sample was then dried under vacuum at 215–220°C for 24 h. Cure kinetics were monitored at 320 and 350°C via FTIR using a Nicolet Impact 400 FTIR spectrophotometer. Samples were first dissolved in dichloromethane or NMP and then two drops of the solution were placed between two sodium chloride discs. These plates were then placed in a vacuum oven at room temperature to remove the solvent prior to analysis. The lap shear adhesion samples were prepared by producing an E-glass cloth impregnated preform containing 85% (wt.%) polymer which was then carefully dried to remove all volatiles before curing at 75 psi in a hot press at 370°C for 1 h between two chromic acid anodized Ti (6/4) adherends. An Instron 1213 was used to test the samples at room temperature following ASTM-D1002, with a crosshead speed of 0.05 in./min.

2.4. Polymer synthesis

A representative synthesis of controlled M_n, 5000 g/mol oligomers is described as follows: Into a four-necked, 250 ml round-bottomed flask fitted with a reverse Dean-Stark trap, a mechanical stirrer, a nitrogen inlet, and a thermocouple port was added 7.040 g (0.031 mol) of bisphenol-A, 8.000 g (0.028 mol) of DCDPS, and 4.908 g (0.036 mol) of K_2CO_3. NMP (55 ml) and toluene (30 ml) were then added and the reaction flask immersed in an oil bath. The reaction temperature was then raised to 145°C where it was maintained with stirring for 6 h then raised to 160°C for 12 h. Next, 2.004 g (0.006 mol) of the endcapper, phenylethynyldiphenylsulfone (PEFDPS), was added along with toluene (30 ml). The reaction was continued for 3 h at 145°C, and for another 6 h at 160°C. Work-up involved filtering the salt by-product, then precipitating the hot filtrate into methanol. The resulting precipitate was dried under vacuum at room temperature, then at a temperature around the glass transition temperature.

3. Results and discussion

A series of 5000 g/mol bisphenol-A and biphenol based oligomers of poly (arylene ether sulfone) endcapped with four different phenylethynyl moieties which contained various electron-withdrawing substituents were synthesized by the reaction of the bisphenol with 4,4′-dichlorodiphenylsulfone according to Scheme 1. In general, the polymerization reactions followed the one-pot procedure outlined in Section 2, but the synthetic approach for the 4-bromo-4′-fluorodiphenylsulfone (4-PEPIP) endcapped polysulfone had to be somewhat modified. ^{13}C-NMR analysis of the product of a reaction by the one-pot approach using 4-PEPIP as endcapper did not show any ethynyl carbon peaks. An investigatory reaction between 4-PEPIP and potassium carbonate alone under identical reaction

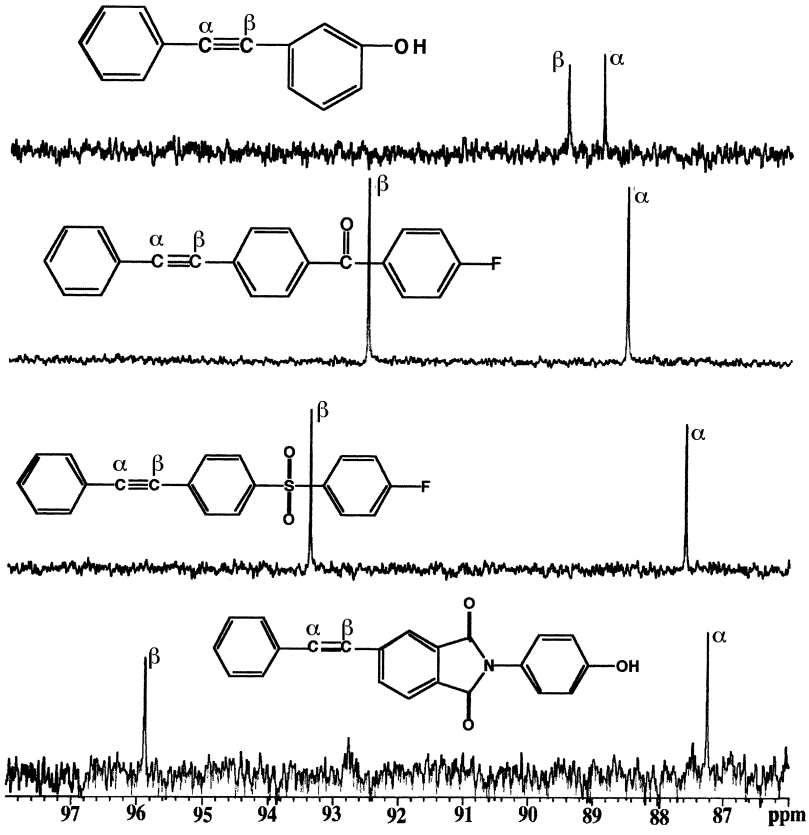

Fig. 1. ^{13}C-NMR spectra of ethynyl region of the endcappers. From top to bottom, 3-PEP, FPEB, PEFDPS, AND 4-PEPIP.

conditions gave primarily phenylethynylphthalic anhydride, indicating that the phthalimide ring undergoes base hydrolysis under those reaction conditions. To circumvent this, a two-step approach was employed by reacting the bisphenol, DCDPS and 3-aminophenol in one step, followed by the reaction of the amine-terminated product with a slight excess of phenylethynyl phthalic anhydride (in NMP/*o*-DCB as imidization solvent). The analogous endcap incorporated into the oligomers thus became 3-PEPIP rather than 4-PEPIP.

The functionally different endcappers employed were PEP, FPEB, PEFDPS, and PEPIP, phenylethynylphenol (PEP) was considered the reference endcapper. The location of the ethynyl carbons in the ^{13}C-NMR gave good indication as to the nature of their electronic environment as illustrated in Fig. 1 [23]. Thus, the trend from PEP to FPEB and PEFDPS down to PEPIP was that the ethynyl carbon atom (C_β) closest to the substituent group, which is expected to be most influenced by it, progressively shows a higher chemical shift, i.e. resonances at increasingly downfield positions. This observation was considered to be a good measure of the electron-withdrawing abilities of each substituent group, increasing in the order: ether < carbonyl < sulfone < imide. The chemical shift positions of the C_α atoms on the other hand, were found to be progressively shifted in the direction opposite to those of the C_β atoms, i.e. upfield. With the aid of such 2-D NMR techniques as DQ-COSY (correlation spectroscopy) used to correlate 3-bond ^{1}H–^{1}H couplings and the heteronuclear multiple-bond coherence (HMBC), chemical shift resonances were accurately assigned to specific carbon atoms. The HMBC technique correlates ^{13}C–^{1}H coupling, generally through two to three bonds. An example is shown in Fig. 2. Protons 2 and 2′ couple with carbon C-4 providing a signal at the intersection of the perpendicular spectra. Other assignments of atom resonances in based on these couplings are shown.

Table 1 illustrates that the influence of the substituent groups on the endcapper extends far beyond the ethynyl carbon atoms. Thus, carbon atoms C-4, C-3 (C-3′), C-2 (C-2′), and C-1 were all progressively shifted upfield, downfield, upfield, and then downfield, respectively, a result which is interpreted as being due to resonance effects. However, neither the resonance, ring currents nor the long-range inductive effects can explain some of the other observations of these systems. A careful inspection of the data in Table 1 reveals that the substituent on the phenyl ring attached to C_β is able to shift electron density from the terminal phenyl ring (attached to C_α), onto the C-4–C_α bond while at the same time shifting electron density away from the C_β–C-5 bond, and into the ring to which it is directly attached. Thus, with increasing electron-withdrawing ability of the substituent, the atoms C-4 and C_α experience progressively increased shielding while C_β and C5 experience progressively increased deshielding. This is

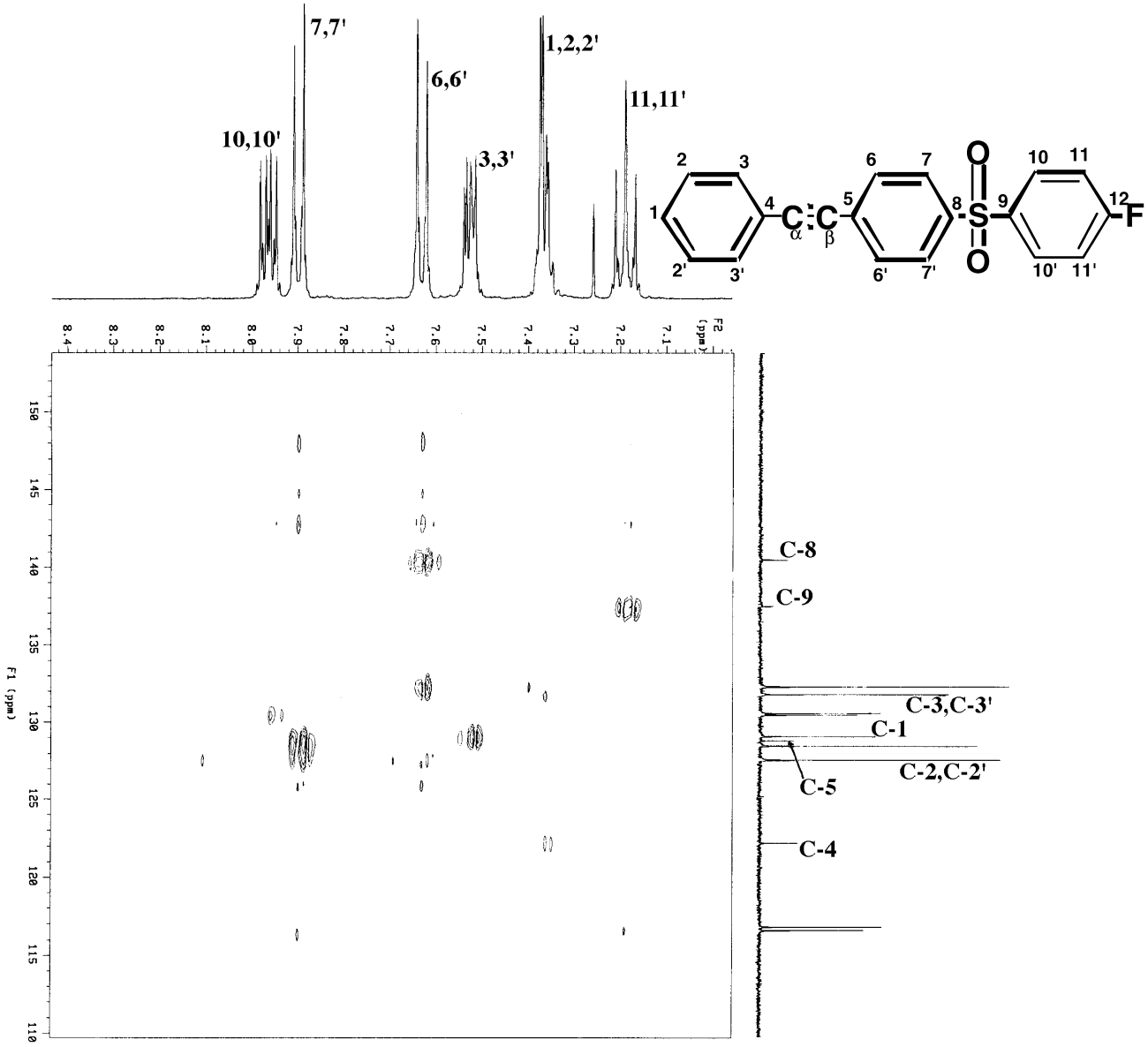

Fig. 2. HMBC-NMR correlation spectrum of PEFDPS.

illustrated in structure **1**.

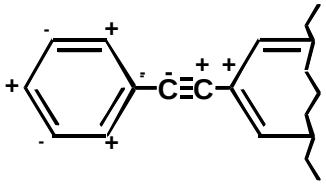

where + = progressive deshielding
- = progressive shielding

1

Here + denotes progressive deshielding and − progressive shielding. In addition, the difference in chemical shift positions (Table 2) of C_α and C_β becomes increasingly larger, i.e. the ethynyl bond appears to become increasingly "polarized". It is interesting to further note that the difference in resonance positions of C-4 and C_α on the one hand, and C_β and C-5 on the other, remains fairly constant, the standard deviations of the differences in chemical shift values between each set of atoms being 34.39 ± 0.26 and 34.73 ± 0.76 ppm, respectively. The implication of this is that both C-4 and C_α, and C_β and C-5 become shielded and deshielded similiarly. The same trends were observed in the resonance positions of the oligomer endgroups although the magnitude of chemical shift differences induced by the electron-withdrawing substituent was much less. A simple inductive effect should diminish with the distance from the electron donor/withdrawer. To the best of our knowledge, there has not been any report of this phenomenon in the literature and

Table 1
^{13}C NMR chemical shift assignments of phenylethynyl-endcappers

Endcapper	Endcap acronym	C-1	C-2 & C-2′	C-3 & C-3′	C-4	C_α	C_β	C-5
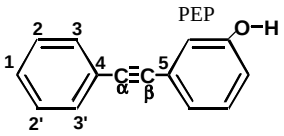	PEP	[a]	128.3	131.6	123.1	88.9	89.4	124.4
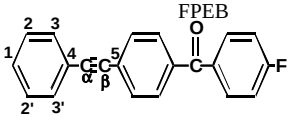	FPEB	128.8	128.4	131.7	122.6	88.5	92.5	127.6
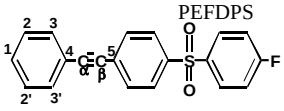	PEFDPS	129.1	127.6	131.8	122.2	87.6	93.4	128.8
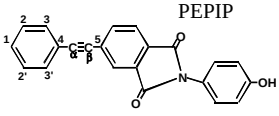	PEPIP	129.7	127.4	132.1	121.9	87.2	95.9	129.3

[a] An accurate assignment of this carbon atom could not be made.

work is currently under way with a view to determining how these electronic effects influence the direction of the curing mechanism. Some model studies will be reported in a future paper [17].

3.1. Investigation of cure kinetics

The kinetics of the curing reactions assume that the reactions proceed by a free-radical mechanism to a large extent. Accordingly, CAChe molecular models for endcapper radical susceptibility using molecular mechanics (MM) for geometry optimization and the Austin Model (AM1) for wave function gave results that are shown in Fig. 3. The surface attributes are such that the lighter colored areas on the molecule have a greater susceptibility to radical attack. As can be seen, apart from PEPIP, susceptibility to radical attack is generally centered around the ethynyl carbon atoms and in addition, susceptibility decreases in going from 3-PEP to FPEB to PEFDPS. This is the exact order of increasing electron-withdrawing ability of substituents as deduced from the ^{13}C resonance positions of the ethynyl carbons in Fig. 1. The surface profile for PEPIP was quite unexpected, as the most susceptible sites to radical attack, as calculated by MM and AM1, were not around the ethynyl bond, but around the phthalimide ring. To find how these modeling results correlate with experimental data, kinetic studies of the curing reaction of the phenylethynyl endcapped 5000 g/mol bisphenol-A based polymers were designed to investigate the effect of the electron-withdrawing ability of a substituent on the rate of the cure reaction. The materials were cured at two different temperatures, 320 and 350°C, and FTIR was used to monitor the curing reaction. The molecular modeling results earlier mentioned, which revealed the ethynyl bonds to be the most probable sites for radical attack, suggested monitoring the time-dependent variations in the intensity of the –C≡C– stretching vibration peak at around 2216 cm^{-1} as a good measure of the progress of the curing reaction. The area of the ethynyl peak was computed with time at a constant temperature and each spectrum was normalized based on the first spectrum of the series. The data were plotted for an apparent first and second-order disappearance in order to determine the best fit [24]. The intensities of the ethynyl peaks increased with the electron-withdrawing ability of the substituent group on the phenylethynyl moiety. This is consistent with the known proportionality of the intensity of IR stretching absorbance of an ethynyl bond with its polarizability.

Table 2
Differences in ^{13}C NMR chemical shift positions of specific endcapper atoms

Endcapper	C-4-C_α	C_β–C_α [a]	C-5–C_β
3-PEP	34.20	0.56 (2.03)	34.97
FPEB	34.06	4.01 (3.48)	35.10
PEFDPS	34.58	5.80 (5.03)	35.41
PEPIP	34.70	8.64 (6.82)	33.45

[a] Values in bracket are those for the oligomer endcappers.

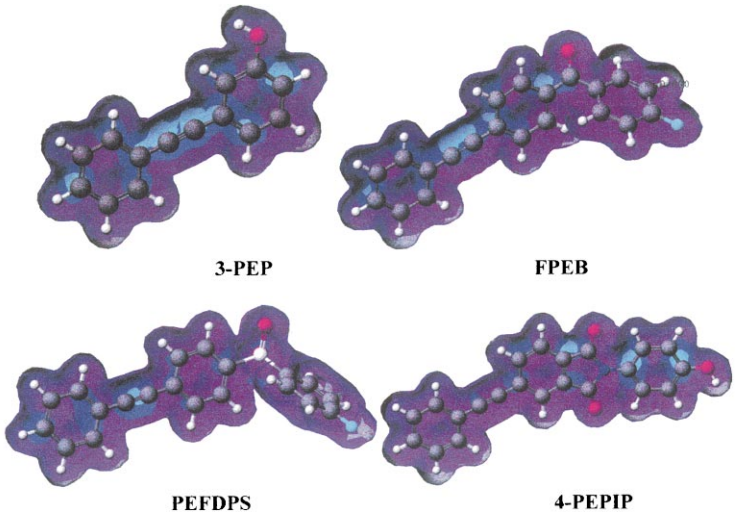

Fig. 3. Molecular models of radical susceptibility sites on phenylethynyl-terminated. endcappers.

Table 2 shows the polarization of the ethynyl bond increasing with electron-withdrawing ability of the substituent group.

Figs. 4 and 5 provide the first- and the second-order rate plots for a PEPIP endcapped polysulfone. Correlation coefficient values of 0.965 (R^2, Fig. 4) and 0.989 (R^2, Fig. 5) or the first-order and second-order rate plots at 350°C, respectively, suggests that a second-order model provides the better fit. This same trend was also observed when the intensities of the ethynyl peak of PEFDPS were monitored and plotted with time (Fig. 6). Subsequently, only the second-order plots are therefore herein. There was, indeed, considerable scatter in the plotted data obtained from the FPEB and 3-PEP-terminated oligomers at both 350 and 320°C, which was probably a result of the lower intensities of their respective ethynyl peaks. This difference in intensities is best illustrated when the stacked spectra of PEFDPS and FPEB-terminated polysulfones (Figs. 7 and 8, respectively) are compared. Clearly, the peaks corresponding to the FPEB-terminated oligomers are considerably less intense, which is, as expected, a consequence of the lower polarizability of the ethynyl bond (Table 2). Reliable data could therefore not be obtained for these systems.

In general, as seen in Figs. 9 and 10 for the PEPIP and the PEFDPS-terminated systems at 320°C, the lower curing temperatures produced greater scatter and lower correlation coefficients. The apparent rate constants for these curing reactions as computed from our FTIR system are shown in Table 3 (a best fit straight line could not be drawn for the PEFDPS oligomer at 320°C).

The above results appear to support the conclusion arrived at by Johnson et al [18], that greater electron-withdrawing

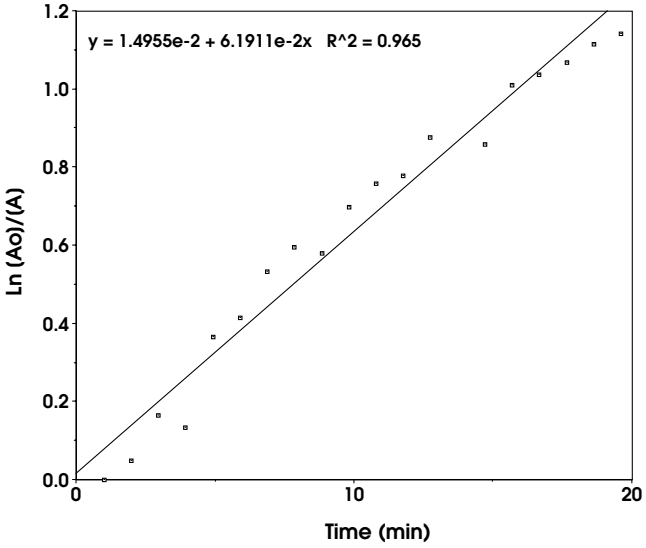

Fig. 4. First-order rate plot of the time-dependent disappearance of the ethynyl. Stretching peak (at 350°C) of the imide-endcapped (PEPIP) polysulfone oligomer

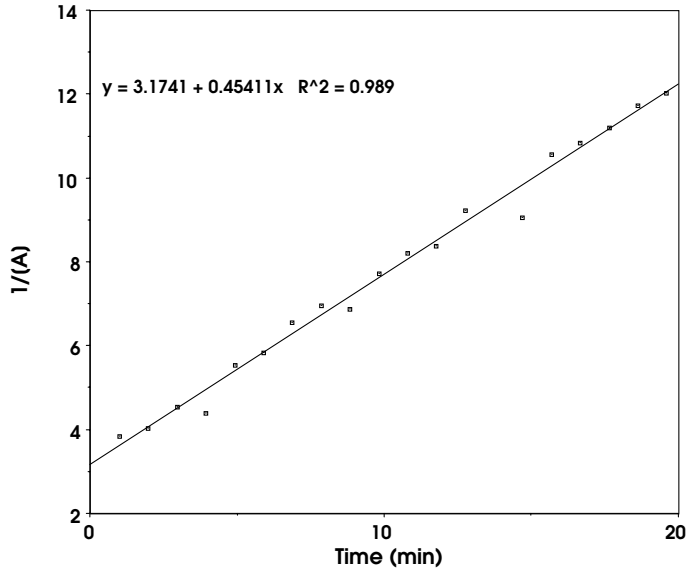

Fig. 5. Second-order rate plot of the time-dependant disappearance of the ethynyl. Stretching peak (at 350°C) of the imide-endcapped (PEPIP) polysulfone oligomer.

ability of the substituent on the phenylethynyl moiety of a particular oligomer produces faster cure rates. In addition, they also suggested that all the curing reactions to a good extent follow the second-order reaction kinetics. Cure kinetics at 370°C could not be followed because the disappearance of the ethynyl stretching absorption peak at that temperature was too rapid for the methodology employed.

These results correlate well with the computer-aided molecular modeling of radical susceptibilty surfaces generated for the various endcappers (Fig. 3). For simplicity, one can focus on the unreacted phenylethynyl endcappers. If initiation of the cure reaction is assumed to occur via the thermally induced generation of free radicals, possibly by cleavage of an ethynyl π-bond, then it is reasonable to expect that this step would be better facilitated if there was an electron-donating substituent attached to the adjacent phenyl ring, because of the increased electron density in the ring π-electrons (Scheme 2) would ensure better resonance stabilization of the resulting ethynyl radical [25]. This ring-facilitated resonance stabilization would require the overlap of the p orbitals of the single electron-occupied C_β and that of C-5 (the phenyl ring therefore contributes an electron through C5), affording an allene-like species **6** (Scheme 3) of perhaps a transitory existence

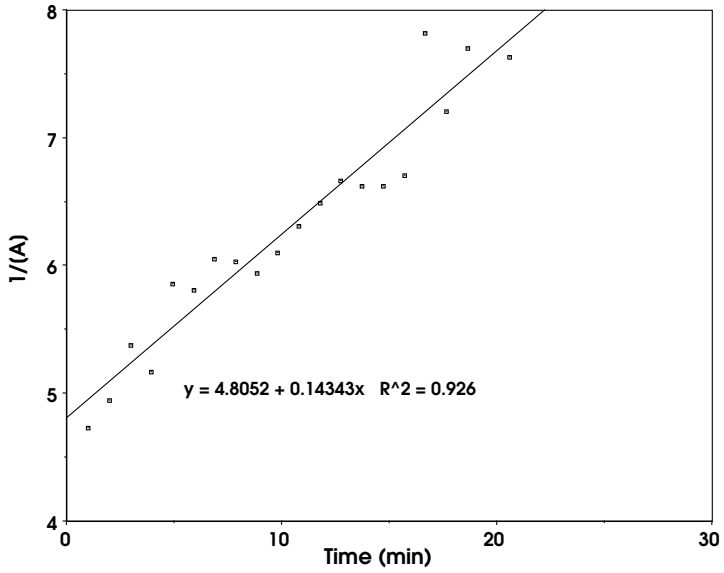

Fig. 6. Second-order rate plot of the time-dependant disappearance of the ethynyl. Stretching peak (at 350°C) of the sulfone-endcapped (PEFDPS) polysulfone oligomer.

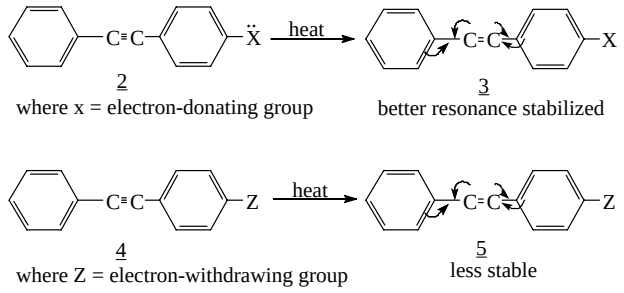

Scheme 2.

(no peak around 1950 cm^{-1}, corresponding to the allene anti-symmetric stretching vibration, was observed in the IR during cure monitoring). An identical scenario would of course be taking place between C-4 and C_α which, if occurring simultaneously with the overlap of C_β and C-5, would give rise to a species with three cumulative double bonds between the two phenyl rings. There is the literature evidence for aryl radicals stabilizing adjacent acetylene bonds as well as for the formation of allenes from acetylenes at elevated temperatures [26]. Hybridization and maximum orbital overlap restrictions would require that each successive double bond be orthogonal to its neighbor, the result of which is that the two phenyl rings on either side of the allene system would be co-planar. Radical stabilization through the two rings would therefore be mutually exclusive with the inner allene double bonds acting as conjugation insulators. Based on results from the present study, it is suggested

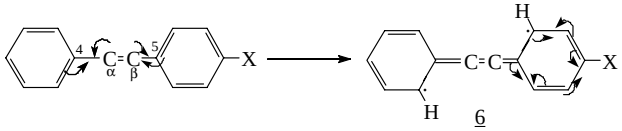

Scheme 3.

that the cure kinetics are governed to a large degree by the delocalizability across C_β and C-5 in particular. An electron-donating substituent on the adjacent phenyl ring would increase electron density across the C_β/C-5 bond and would therefore better facilitate the stabilization of a radical at C_β. One should recall from the ^{13}C NMR data that electron density across this bond progressively decreases with increasing electron-withdrawing ability of the substituent on the adjacent phenyl ring. Thus, electron-donating substituents would facilitate the initiation step whereas electron-withdrawing substituents would hinder it. However, the fact that the resulting new radical is well stabilized by the electron-donating substituent would in turn, hinder that radical from any further reaction, e.g. propagation. The converse of this is true, i.e. although electron-withdrawing substituents suppress the generation of radicals on the ethynyl bond, once formed, those radicals react faster due to their comparatively reduced stability (Scheme 4). This further reaction of the radical species corresponds to propagation/termination steps that likely follow the second-order kinetics. Therefore, in a situation where a variety of molecules containing phenylethynyl groups about to undergo

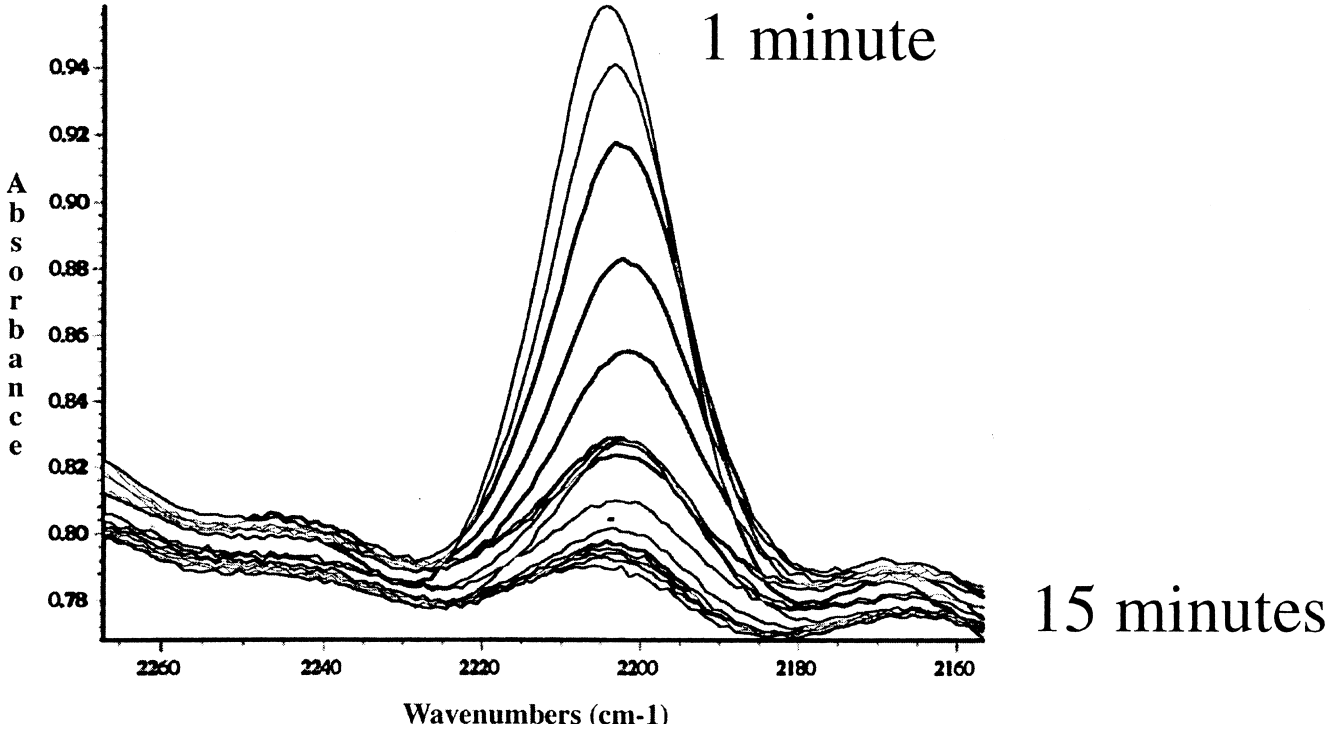

Fig. 7. FTIR spectra of a 5000 g/mol bisphenol A based PEFDPS polysulfone oligomer taken every 1 min at 350°C.

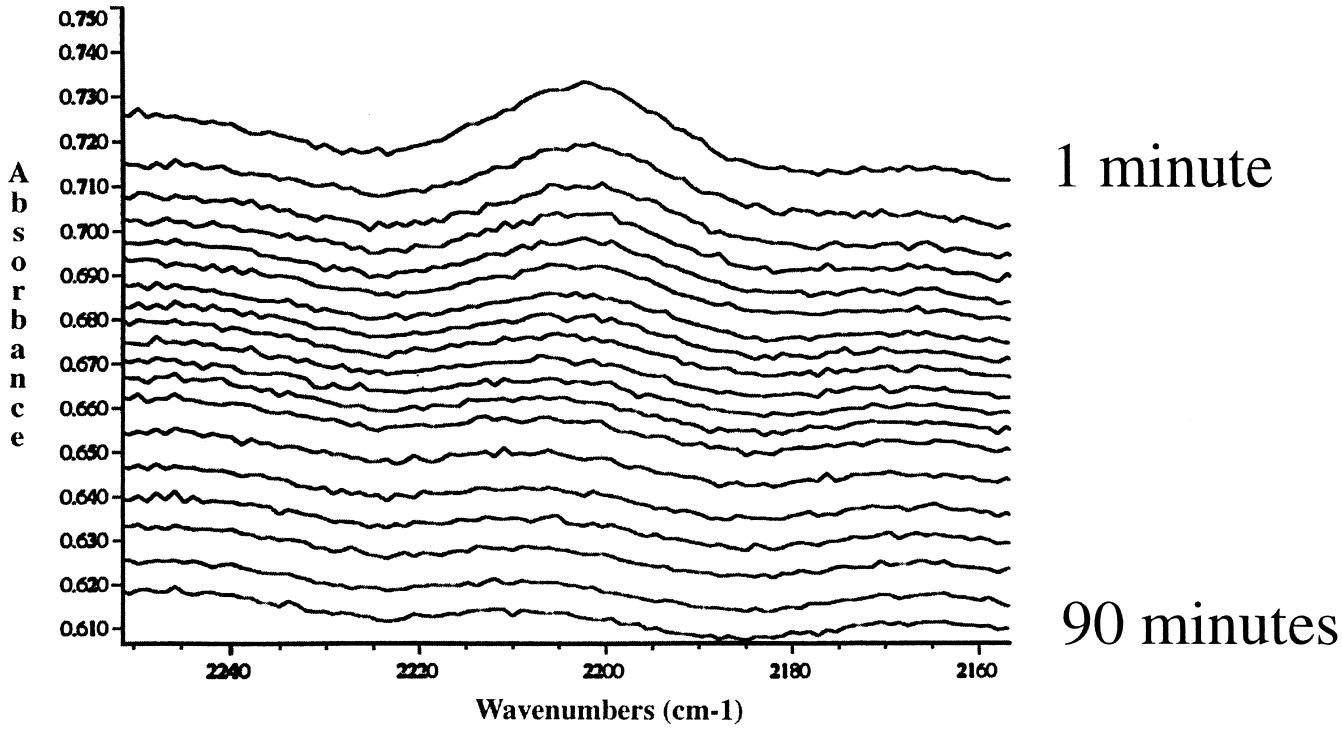

Fig. 8. FTIR spectra of a 5000 g/mol bisphenol A based PEFDPS polysulfone oligomer taken at selected times.

radical reaction, it is hypothesized that those that have electron-donating substituents will initiate faster, but will propagate/terminate slower. If the reaction temperature is high enough such that sufficient energy is available to overcome the activation energies for the initiation steps of all the different phenylethynyl-endcappers, then the rate of reaction becomes very dependent on the propagation/termination steps, both of which are proposed to be second-order, and both of which will be accelerated by electron-withdrawing substituents. This explanation appears to be consistent with our experimental results.

3.2. Solubility characteristics

The bisphenol A based oligomers were all readily soluble in chloroform whereas the biphenol-based oligomers were not. All oligomers (both Bis A and biphenol based) were nevertheless soluble in both NMP, and in a 95% $CHCl_3$/TFA [26,27] solvent system. The limited solubility of the biphenol-based oligomers can be attributed to their partially semi-crystalline morphology. The solubility of the semicrystalline oligomers in the $CHCl_3$/TFA solvent system is probably due to a disruption of crystallinity by the added TFA. This may occur via the formation of clusters of hydrogen bonded TFA which are also hydrogen-bonded to the sulfone oxygen atoms of the polysulfone chain, thus disrupting the order between oligomeric units (Fig. 11). Although there is no direct evidence for this, Eisenbach and Sperlich [28] have shown the possibility of this scenario in nitrile systems.

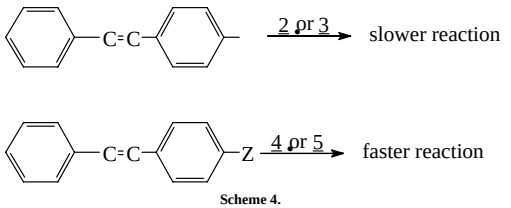

Scheme 4.

Scheme 4.

3.3. Molecular weights and thermal analysis

Molecular weight determinations were conducted by quantitative size exclusion chromatography (SEC) [29] and by quantitative ^{13}C NMR analysis of the endgroups as shown in Table 4. In general, molecular weights computed by the endgroup analysis were higher than those obtained from SEC measurements, but the values were within the error levels expected for the two measuring techniques. Absolute calculation of molecular weight is less accurate with low-molecular-weight samples than with higher-molecular-weight samples. The difficulty arises due to the separation of very low-molecular-weight oligomers that elute very near to the solvent peak in NMP. The calculation in the lower-molecular-weight region is therefore less accurate than in the higher-molecular-weight region. Assuming that the statistical distribution for the step-growth polymers is 2.0 and dividing the weight average molecular weight by 2, may give a more accurate number for the number average molecular weight. The distributions of all the oligomers

Table 3
Apparent second-order rate constants at 320 and 350°C for phenylethynyl terminated oligomers cured between NaCl disks in the FTIR

Endcapper	k at 320°C (s^{-1})	k at 350°C (s^{-1})
PEFDPS		0.14
PEPIP	0.24	0.45

used in this research were similar with no major variations between samples.

Table 5 shows that the T_gs of the oligomers were similar, as any variation can be attributed to the slight differences in molecular weights below the entanglement molecular weight. The higher T_gs of the biphenol-based oligomers is a consequence of the more rigid chains. It was also observed that the low gel fractions and T_g values of the cured thermosets resulting from the 3-PEPIP imide terminated polysulfones appeared to be anomalous when the general trend is considered.

Dynamic thermal gravimetric analysis (TGA) (Fig. 12) showed, as expected, that the biphenol-based systems exhibited temperatures of 5% weight loss higher than those of the isopropylidene containing bisphenol-A systems. Curing was conducted in an aluminum mold under nitrogen at 370°C for 2 h. The cured materials all formed creasable films and gel fractions were highest for the bis-A-based

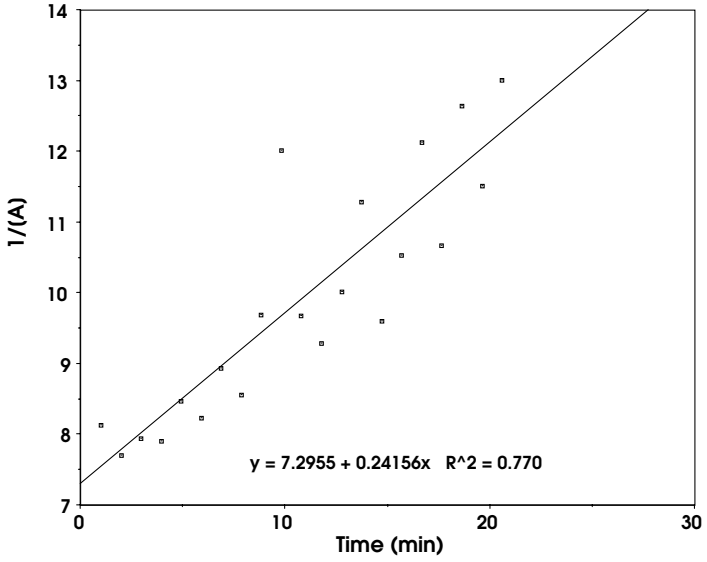

Fig. 9. Second-order rate plot of the time-dependant disappearance of the ethynyl. Stretching peak (at 320°C) of the imide-endcapped (PEPIP) polysulfone oligomer.

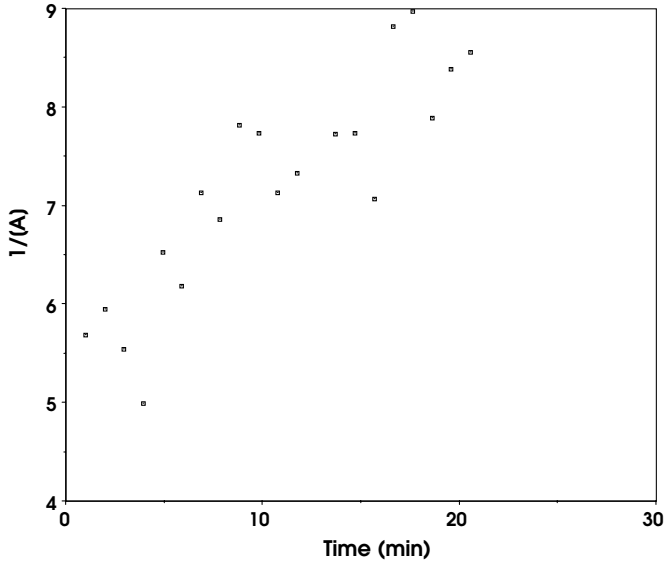

Fig. 10. Second-order rate plot of the time-dependant disappearance of the ethynyl. Stretching peak (at 320°C) of the sulfone-endcapped (PEFDPS) polysulfone oligomer.

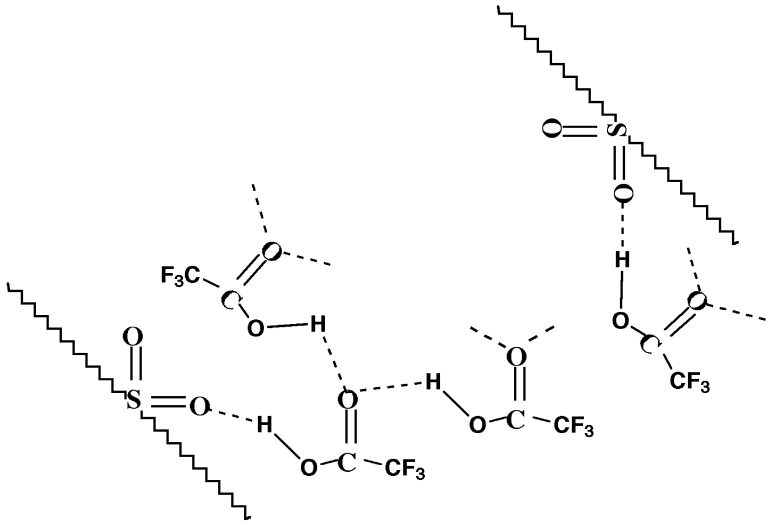

Fig. 11. Representation of possible hydrogen-bonded clusters of TFA disrupting the order between biphenol-based oligomeric chains.

Table 4
Molecular weight characterization of phenylethynyl poly(arylene ether sulfone) oligomers (target = 5000 g/mol)

Oligomer/endcap	M_n[a] (GPC) g/mol	M_w (GPC) g/mol	M_w/M_n	M_n ^{13}C NMR
Bis A/3-PEP	4500	9800	2.18	5500
Bis A/FPEB	4600	8300	1.84	6200
Bis A/PEFDPS	4000	7000	1.76	5500
Bis A/3-PEPIP	6000	9900	1.74	6000
BP/3-PEP	5300	9300	1.75	5300
BP/FPEB	6700	11,100	1.65	7900
BP/PEFDPS	6800	10,700	1.58	7700
BP/3-PEPIP	6000	9200	1.52	5000

[a] Run in NMP with 0 02 mol% P_20_5 at 60°C.

Table 5
Thermal analysis and gel fractions of phenylethynyl poly(arylene ether sulfone) oligomers

Oligomer	M_n[a] (GPC) g/mol	Oligomer T_g[b] (°C)	5% wt loss, °C (TGA)[c]	% Gel fraction[d]	T_g (°C) [e] cured	Δ T_g[f] (°C)
Bis A/ 3-PEP	4500	153	491	91	198	8
Bis A/ FPEB	4600	166	514	97	206	16
Bis A/ PEFDPS	4000	162	498	97	215	25
Bis A/ 3-PEPIP	6000	165	504	85	200	10
BP/ 3-PEP	5300	184	549	90	234	4
BP/ FPEB	6700	207	542	90	240	10
BP/ PEFDPS	6800	206	525	91	243	13
BP/ 3-PEPIP	6000	191	521	88	235	5

[a] In NMP at 60°C, Target M_n = 5000 g/*mol*.
[b] Second heat, run at 10°C/min after heating to 280°C, then quenching.
[c] Run at 10°C/min.
[d] Extracted with $CHCl_3$ for 96 h and dried at 215–220°C for 24 h.
[e] Second heat, run at 10°C/min after heating to 400°C, then quenching.
[f] Cured $T_g - T_g$ of high-moleuclar weight thermoplastic.

thermosets. The highest T_g obtained for the cured networks was 243°C (for the biphenol-based PEFDPS endcapped polymer), nearly as high as the 250°C target. One observes that the M_n obtained by SEC in that case is 6800 g/mol suggesting that if a lower-molecular-weight oligomer M_n were prepared, the T_g could approach, or even surpass the goal of 250°C, because of the higher network density. The ΔT_g is reported as the difference in temperature between the

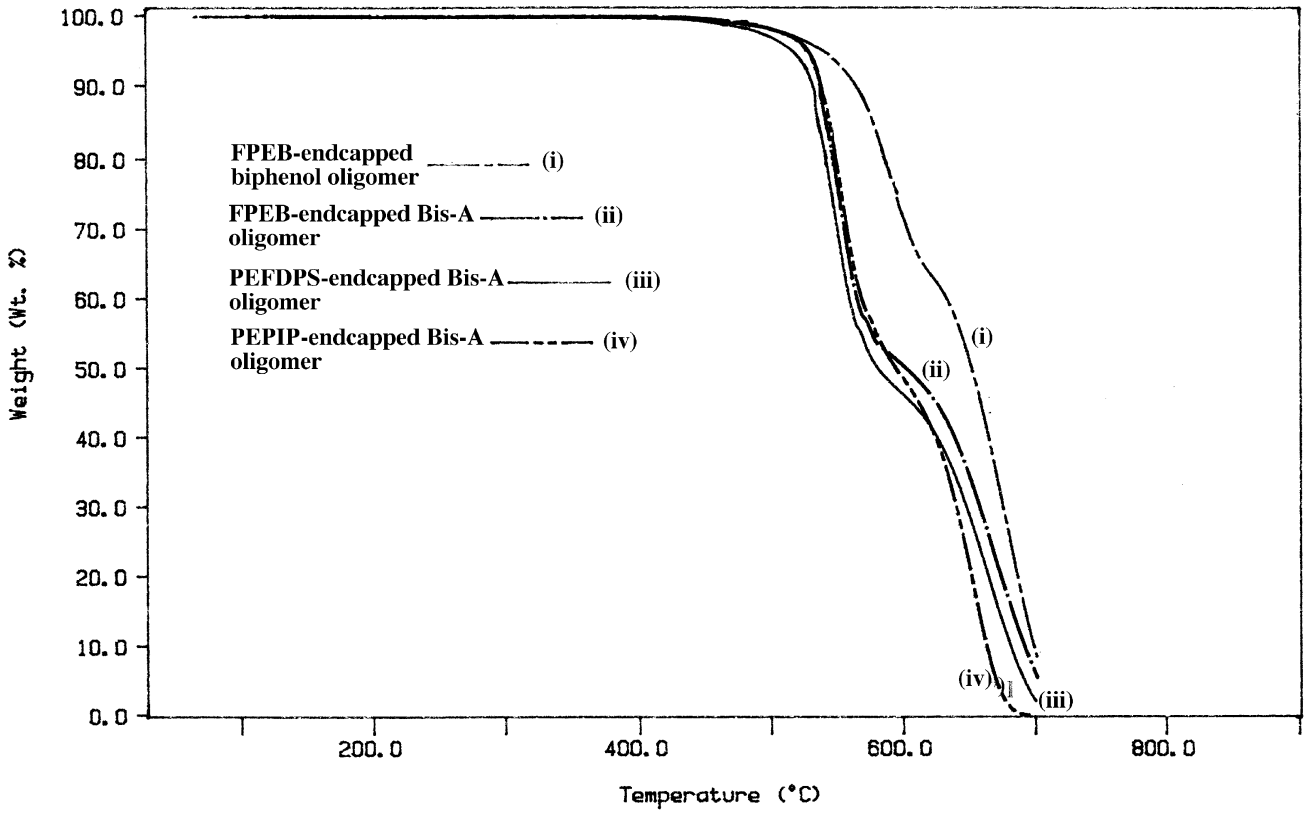

Fig. 12. TGA thermogram of phenylethynyl terminated poly(aryelene ether sulfone).

cured thermoset T_g and the high-molecular-weight thermoplastic T_g. A large increase in T_g is expected with high network density. The failure of the cured phenylethynylphenol endcapped polymers to demonstrate a significant increase in the glass transition temperature over the linear thermoplastic led to this study of varied endcappers. Further studies are in progress. The pattern that develops is that the T_g of the thermoset appears to increase in the order of electron-withdrawing ability of the substituent in the endgroup, with the only anomaly being the imide endcapped polymers. The increase in the ΔT_g is also clear except in the case of the imide endcapped oligomers. Higher gel fractions are expected to lead to more of an increase in the T_g, this is seen in the comparison of the two polymer systems where the bisphenol A polymers exhibit both higher gel fractions and larger ΔT_gs.

Table 6
Single lap shear results for cured oligomers with different phenylethynyl endcappers

Bisphenol	Endcapper	Adhesive strength,[a] psi (MPa)
Bisphenol A	PEP	3850 ± 470[b] (26.5 ± 3.2)
	FPEB	4680 ± 260 (32.3 ± 1.8)
	PEFDPS	4890 ± 520 (33.7 ± 3.6)
	PEPIP	5090 ± 510 (35.1 ± 3.5)
4,4′-biphenol	PEP	4090 ± 250 (28.2 ± 1.7)
	FPEB	4890 ± 580 (33.7 ± 4.0)
	PEFDPS	5330 ± 220 (36.7 ± 1.5)
	PEPIP	5230 ± 310 (36.1 ± 2.1)

[a] Average of four samples, cured at 370°C/120 min, chromic acid anodized, cohesive failure.

[b] Average. of four samples, cured at 370°C/90 min, pasa jel treatment, cohesive failure.

The single lap shear adhesion to titanium results are presented in Table 6, for the phenylethynyl terminated polysulfone thermosets. The sample for the bisphenol A based 3-PEP themoset was prepared using a Pasa Jel surface treatment which in our hands provides consistently lower adhesion strengths than the chromic acid anodized surface treated samples. The relatively lower adhesion strengths of the phenylethynylphenol-based materials are noted. A consistent difference is present in the carbonyl and sulfone based materials as well and the imide based material is about the same as the sulfone even though the gel fractions and T_g are lower. Failure of the adhesive bonds was cohesive and from the DMA results for the bis A-based thermosets shown in Fig. 13 do correlate well with the approximate elastic modulus above T_g.

The adhesion values did correlate with modulus above T_g (which is proportionally related to the crosslink density of the material [30,31]) for each of the thermosets. Thus, the 3-PEP endcapped material which had the lowest adhesion strength also had the lowest modulus above the T_g. These lap shear strengths are much higher than earlier determined for the phenylethynyl polysulfone materials [13] and are comparable with phenylethynyl terminated polyimides [15]. The resistance to possible strongly basic environments

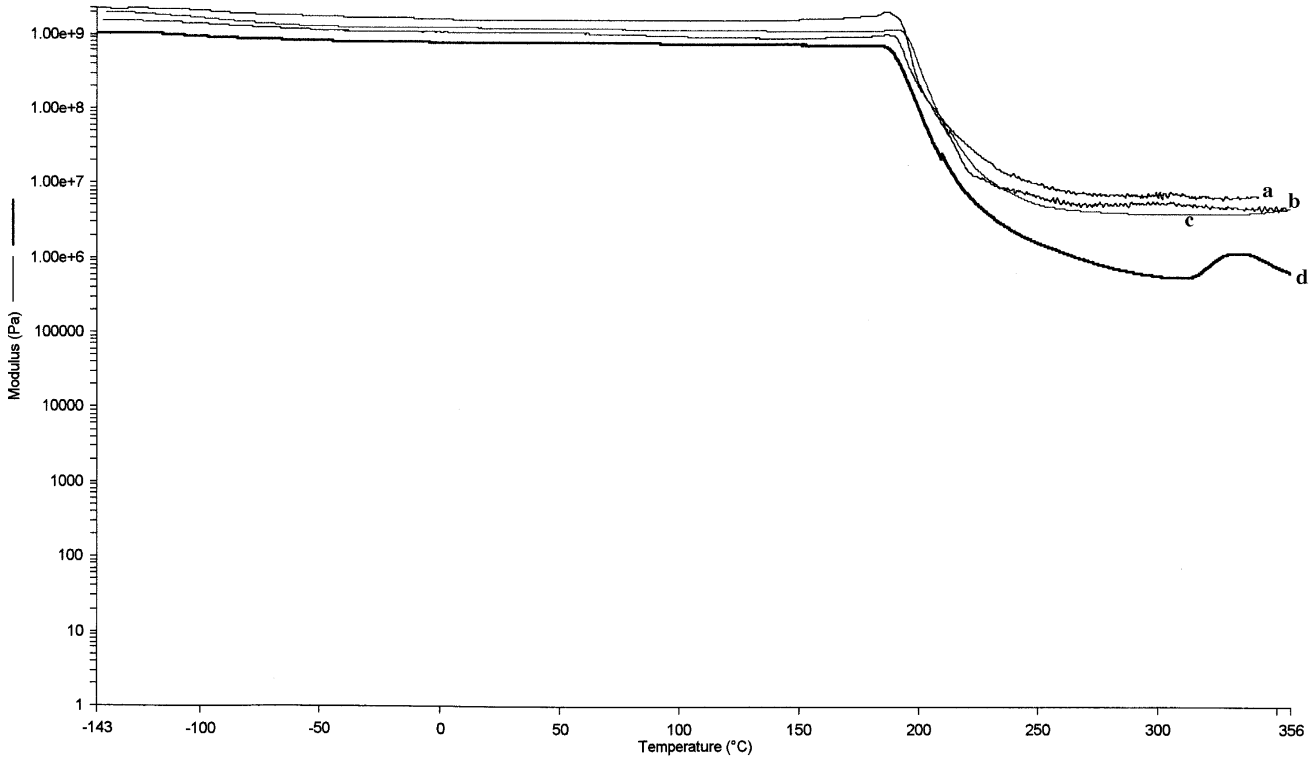

Fig. 13. DMA thermogram of poly(arylene ether sulfone) thermosets: (a) PEFDPS terminated; (b) FPEB terminated; (c) 3-PEPIP terminated; (d) PEP terminated.

should be much better for the polyarylene ethers. These results indicate that an increased reactivity and crosslink density could be important to the adhesion strength to metal adherends.

4. Summary and future studies

Poly(arylene ether sulfones) terminated with various phenylethynyl groups were prepared which differed in the electron-withdrawing abilities of the substituents on the reactive endgroup. It has been established through NMR and FT-IR that the nature of the phenylethynyl endgroup, specifically, the electron-withdrawing ability of an attached substituent plays a major part in the kinetics and likely the mechanism of the curing reaction. Glass transition temperatures, modulus above T_g, and adhesion strengths of the resulting thermosets were found to, in general, increase with increased electron-withdrawing ability of the substituent on the endcapper. Continuing efforts are currently focused towards further elucidating the complex reaction mechanisms involved in curing reactions, as well as the application of these materials as composite matrix resins and adhesives.

Acknowledgements

The authors would like to thank the Adhesive and Sealant Council Education Foundation and the NSF Science and Technology Center: High Performance Polymeric Adhesives and Composites (DMR-9120004) for the financial support of this work. Drs Qing Ji and M. Sankarapandian provided excellent SEC and adhesion analyses, respectively. Generous support from the GenCorp Foundation is acknowledged.

References

[1] Johnson RN, Farnham AG. J Polym Sci A-1 1967;5:2415.
[2] McGrath JE, Farnham AG, Robeson LM. Polym Prepr 1975;16(1):476–482.
[3] McGrath JE, Farnham AG, Robeson LM. Appl Poly Sci, 1975: symp no. 26.
[4] Robeson LM, Farnham AG, McGrath JE. In: Meier DJ, editor. Midland Macromolecular Institute monographs. London: Gordon and Breach, 1978. p. 405–526.
[5] Viswanathan R, Johnson BC, McGrath JE. Polymer 1984;25:1827.
[6] Hedrick JL, Mohanty DK, Johnson BC, Viswanathan R, Hinkley JA, McGrath JE. J Poly Sci: Polym Chem Ed 1986;23:287.
[7] Hergenrother PM. Angew Chem Int Ed Engl 1990;29:1262.
[8] Mecham S, Vasudevan V, Liu S, Bobbitt MB, Srinivasan S, Loos AC, McGrath JE. Polym Mater Sci Engng Proc 1996;74:61.
[9] Meyer GW, Tan B, McGrath JE. High Perform Polym 1994;6:423.
[10] Meyer GW, Pak SJ, Lee YJ, McGrath JE. Polymer 1995; 36(11):2303.
[11] McGrath JE, Meyer GW. US Patent no 5,493,002, 1996.
[12] Hergenrother PM, Smith Jr. JG. Polymer 1994;35(22):4857.
[13] Mecham SJ, Bobbitt MM, Pallack ME, Vasudevan V, McGrath JE. Adh Soc Proc 1997;211.

[14] Mecham SJ, Bobbitt MM, Pallack ME, Vasudevan V, McGrath JE. Adh Soc Proc 1997;33.
[15] Tan B, Tchatchoua CN, Vasudevan V, Dong L, McGrath JE. Polym Mater Sci Engng Proc 1998;35(9):84.
[16] Meyer GW. PhD Dissertation, VPI and State University, 1995.
[17] Holland TV, Glass TE, McGrath JE. Polymer 2000;41:4965.
[18] Johnson JA, Li FM, Harris FW, Takekoshi T. Polymer 1994;35(22):4865.
[19] Hergenrother PM. Trends Polym Sci 1996;4(4):104.
[20] Cotter RJ. Engineering plastics: a handbook of polyarylethers. London: Gordon and Breach, 1995.
[21] Hedrick JL, Mohanty DK, Johnson BC, Viswanathan R, Hinkley JA, McGrath JE. J Polym Sci : Polym Chem Ed, vol. 23, 1986. p. 287.
[22] Johnson RN, Farnham AG, Clendinning RA, Hale WF, Merriam CN. J Polym Sci A-1 1967;5:2375.
[23] Mecham SJ. PhD Dissertation, VPI & State University, 1997.
[24] Levine IN. Physical chemistry, 3rd edn. New York: McGraw-Hill, 1988.
[25] Pignaniol P. Acetylene homologs and derivatives. 1st 1950;92–105.
[26] Hariharan R, Pinkus AG. Polym Bull 1993;30:91.
[27] Ayambem A, Pinkus AG. Polym Prepr 1996;31(1):437.
[28] Eisenbach CD, Sperlich B. Macromolecules 1996;29:7748.
[29] Konas M, Moy TM, Rogers ME, Schultz AR, Ward TC, McGrath JE. J Poly Sci: Polym Phys 1995;33:1441.
[30] Levita G, De Petris S, Marchetti A, Lazzeri A. J Mater Sci 1991;26:2348.
[31] Urbaczewski-Espuche E, Galy J, Gerard J, Pascault J, Sautereau H. Polym Eng Sci 1991;31(22):1572.